

# **Instability of Rotational and Gravitational Modes of Oscillation**

By

T. J. Simons and Desiraju B. Rao

Department of Atmospheric Science  
Colorado State University  
Fort Collins, Colorado

**Colorado**  
**State**  
University

**Department of**  
**Atmospheric Science**

Paper No. 155

INSTABILITY OF ROTATIONAL AND  
GRAVITATIONAL MODES OF OSCILLATION

by

T. J. Simons

and

Desiraju B. Rao

This research was supported by

NSF GA-11637

U.S.A.F. F 19628-68-C-0104

Department of Atmospheric Science  
Colorado State University  
Fort Collins, Colorado

January 1970

Atmospheric Science Paper No. 155

## TABLE OF CONTENTS

	<u>Page</u>
Abstract	
1. Introduction	1
2. Characteristic Equation	2
3. Results	5
Case (a): Without rotation	5
Case (b): With rotation	8
4. Summary and Conclusions	18
References	21

Instability of rotational and gravitational  
modes of oscillation

by

T. J. Simons

and

Desiraju B. Rao

Colorado State University

ABSTRACT

The problem of dynamic stability of small amplitude motions on a two-fluid system with a free surface is considered. For the case of no rotation the character of the Kelvin-Helmholtz instability is shown to be different when compared to systems where the external gravitational modes are absent either through the mechanism of filtering or by imposing a rigid top. In the case of a constant rotation, it is shown that the instabilities on a wave length - shear plane consist of regions where only the gravitational modes or only the rotational modes or both independently are unstable, in addition to regions where instabilities are generated by an interaction between the gravitational and rotational modes.

## 1. Introduction.

The purpose of the investigation is to examine the consequences of certain approximations that are normally employed in the studies of large scale atmospheric processes. In order to achieve this end, one may consider perturbations on the following rather simple model. It consists of two incompressible fluids of constant but different densities superimposed one on top of the other in a gravitationally stable configuration on a plane of constant rotation. Each fluid layer has a finite depth and has a constant translational velocity in the positive x-direction. The existence of non-zero velocities in the ground state on a rotating plane brings into play coriolis forces, which then will have to be balanced by counter-acting pressure gradient forces in order to have a balanced initial state. These are generated by the interface between the two fluids, as well as the free surface, sloping away from the horizontal at an appropriate angle.

The problem as stated above may be looked at as a re-formulation of the Kelvin-Helmholtz instability problem on a rotating plane as, for example, considered by Chandrasekhar (1961). However in the latter case, the fluids are of infinite depth so that the perturbations are necessarily non-hydrostatic in their dynamics. In the present formulation of the problem, the perturbation dynamics are hydrostatic since the fluids are of finite depth and the horizontal scales of motions are much larger than the depth scale. Further Chandrasekhar (1961) ignores the interfacial slope required to balance the coriolis forces in the basic state. This slope is responsible for generating the rotational modes of oscillation in a hydrostatic system and cannot be ignored here. Since now the interface and the free surface slope at an angle to the horizontal, we need to insert boundaries in the lateral direction to prevent the interface from

either touching the ground or the free surface. In order to avoid this, we introduce an approximation in which we treat the depths of the fluid layers as constant except when these depths occur in a differentiated form in the governing equations. Approximations of this type are quite common in studies of large scale atmospheric dynamics (Phillips 1951). This approximation makes the coefficients in the governing differential equations constants and since there are no lateral boundaries at which vanishing normal velocity requirements have to be satisfied, one can immediately seek oscillatory solutions to the problem.

In the following sections, we set up the dynamical equations for the perturbations and obtain an equation relating the phase speed  $c$  of the perturbations to other parameters of the problem. This characteristic equation is then analysed under certain approximations. Two aspects of the problem will be considered in particular: (a) the effect of the free surface on the gravitational mode (Kelvin-Helmholtz) instability, and (b) the effects of the internal gravity modes of oscillation on the rotational (quasi-geostrophic) mode instability.

## 2. Characteristic equation

The basic state as described in the preceding section is given by

$$\frac{d\bar{h}_1}{dy} = \frac{f}{g} \frac{\epsilon \bar{U}_2 - \bar{U}_1}{1-\epsilon} \equiv \frac{f}{g} \alpha_1$$

and

(2.1)

$$\frac{d\bar{h}_2}{dy} = -\frac{f}{g} \frac{\bar{U}_2 - \bar{U}_1}{1-\epsilon} \equiv \frac{f}{g} \alpha_2$$

Where  $\bar{h}_1$  and  $\bar{h}_2$  are the depths of the lower and upper layers.  $\bar{U}_1$  and  $\bar{U}_2$  are the speeds in each layer in the ground state and these are taken as constants.  $\epsilon$  is the density ratio ( $\rho_2/\rho_1$ ) and in general  $0 < \epsilon < 1$ ,  $f$  is

the coriolis parameter and  $g$  is the acceleration due to gravity. The dynamical equations for a two-layer quasi-static system are then linearised about this state of equilibrium. The vorticity and divergence equations are now formulated:

$$\begin{aligned} ik(\bar{U}_i - c) \chi_i - f\psi_i + g(h_i + \epsilon_i h_2) &= 0 \\ ik(\bar{U}_i - c) \psi_i + f\chi_i &= 0 \\ ik(\bar{U}_i - c) gh_i + ikf\alpha_i \psi_i - \mu^2 gD_i \chi_i &= 0 \end{aligned} \quad (2.2)$$

Where  $i = 1, 2$  and

$$\epsilon_i = \begin{cases} \epsilon & \text{for } i = 1 \\ 1 & \text{for } i = 2 \end{cases}$$

In equations (2.2)  $\chi$  represents the perturbation velocity potential (or the irrotational part of the velocity field) and  $\psi$  the perturbation stream function (or the solenoidal part of the velocity field).  $h_1, h_2$  are the perturbation heights of the lower and upper layers. It is assumed in (2.2) that all perturbations have the form of plane waves  $\exp. i(kx + \ell y - kct)$ , so that the vorticity and divergence of the velocity field  $\mathbf{W}$  are given by

$$\mathbf{k} \cdot \nabla \times \mathbf{W} = \nabla^2 \psi = -\mu^2 \psi$$

$$\nabla \cdot \mathbf{W} = -\nabla^2 \phi = \mu^2 \phi$$

where  $\mu^2 \equiv (k^2 + \ell^2)$ . In equations (2.2) one minor assumption is incorporated in order to obtain a system of equations with constant coefficients. The assumption is that in the continuity equation, we replace

$$\nabla \cdot (g\bar{h}_i \nabla \chi_i) \approx \nabla \cdot (gD_i \nabla \chi_i) = gD_i \nabla^2 \chi_i$$

where  $D_i$  is the (constant) basic state mean depth of each layer.

It is necessary to make this approximation in this form in order to avoid the introduction of spurious complex roots. The other alternative would have been  $\nabla \cdot (g\bar{h}_i \nabla \chi_i) = gD_i \nabla^2 \chi_i + \nabla g\bar{h}_i \cdot \nabla \chi_i = gD_i \nabla^2 \chi_i + ikf\alpha_i \chi_i$ . The presence of this last term in the equations would then make all roots complex. By comparison with solutions for systems with lateral boundaries, the first alternative seems to offer the best approximation. As mentioned in the Introduction, the basic state slope of the interface and the free surface are still retained in the system of equations by virtue of the term  $ikf\alpha_i \psi_i$  in the continuity equation.

Equations (2.2) represent a set of six homogeneous algebraic equations involving the characteristic value  $c$ , which is determined by the condition that the coefficient determinant be set equal to zero. The resulting characteristic equation may be written in the following non-dimensional form.

$$[\delta_1(1+\tau)^3 - (1+\lambda_1)(1+\tau) + \gamma_1\lambda_1][\delta_2(1-\tau)^3 - (1+\lambda_2)(1-\tau) + \gamma_2\lambda_2] - \epsilon [(1+\tau) - \gamma_1\lambda_1][(1-\tau) - \gamma_2\lambda_2] = 0 \quad (2.3)$$

In this equation, the following non-dimensional parameters have been defined:

$$\lambda_i \equiv \frac{f^2}{\mu^2} \frac{1}{gD_i}$$

$$\delta_i \equiv \frac{k^2}{\mu^2} \frac{(\bar{U}_2 - \bar{U}_1)^2}{4gD_i}$$

$$\tau \equiv \frac{2}{\bar{U}_2 - \bar{U}_1} \left[ c - \frac{\bar{U}_1 + \bar{U}_2}{2} \right]$$

$$\gamma_i \equiv \frac{2}{1-\epsilon} \frac{\epsilon_i \bar{U}_2 - \bar{U}_1}{\bar{U}_2 - \bar{U}_1}$$

From these definitions, it is obvious that  $\tau$  replaces  $c$  as the characteristic value of the problem.

### 3. Results:

In order to keep the analysis simple we consider the special case of equal depths:

$$D_1 = D_2$$

This then makes  $\lambda_1 = \lambda_2$  and  $\delta_1 = \delta_2$ . We now introduce several approximations into (2.3) and investigate their effect on the dynamic stability of the flow.

#### Case (a): Without rotation (gravitational mode instability)

Consider the case of no rotation so that  $\lambda = 0$ . Then the equation (2.3) reduces to

$$[\delta(1+\tau)^2 - 1] [\delta(1-\tau)^2 - 1] - \epsilon = 0 \quad (3.1)$$

This is a bi-quadratic equation representing two external gravitational modes and two internal gravitational modes.

#### Case (a1): Internal gravitational modes only

One can introduce an approximation in (3.1) to filter the external gravity waves without going to the extent of putting a rigid top on the model. If one considers equation (3.1) in the limit of  $\delta^2 \ll 1$ , then we obtain

$$2\delta(\tau^2+1) = 1-\epsilon \quad (3.2)$$

so that the stability criterion in this case may be written as

$$\begin{array}{l} < & \text{stable} \\ \delta & \frac{1-\epsilon}{2} \\ > & \text{unstable} \end{array} \quad (3.3)$$

This criterion shows that instability once realised would persist for all higher values of shear. This may be compared with the case of a two-fluid system with a rigid top.

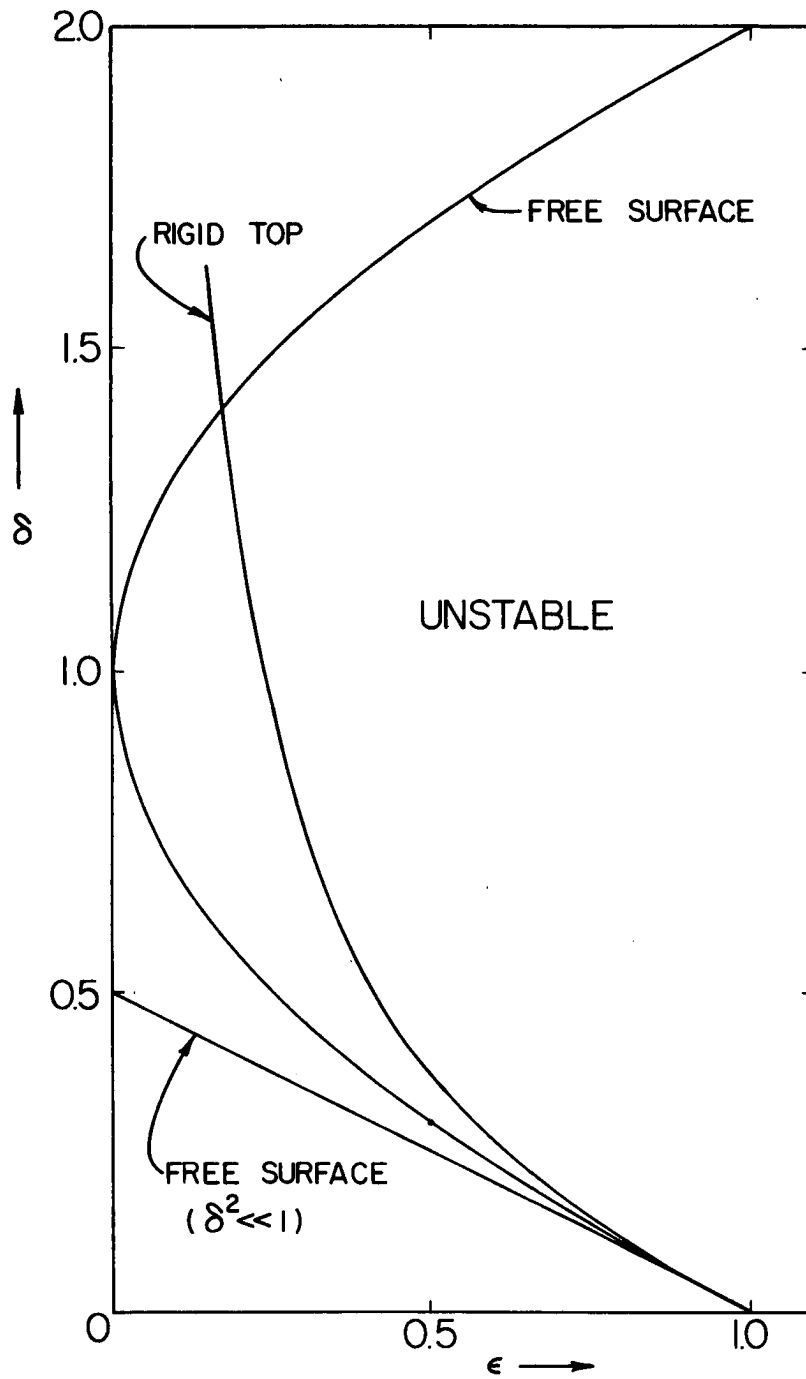


Figure 1. Comparison of the stability properties of the internal gravitational modes. Absissa represents density ratio and the ordinate is proportional to the square of shear.

In the latter case the stability criterion may be stated as (eg. by taking the hydrostatic equivalent of equation 10.31(2) in Godske et al 1957):

$$\begin{array}{l} < & \text{stable} \\ \delta & \frac{1-\epsilon^2}{4\epsilon} \\ > & \text{unstable} \end{array} \quad (3.4)$$

under the assumption  $D_1 = D_2$ . Stability criterion (3.4) also shows that once a critical value of the shear is reached the fluid configuration remains unstable for all shears greater than the critical value.

Case (a2): Internal plus external gravitational modes

An analysis of the complete equation (3.1) shows that the external gravitational modes which correspond to the plus root of the solution for the bi-quadratic are always stable. The internal gravitational modes which correspond to the negative root, on the other hand, can become unstable. The value of  $\tau$  for these internal modes is given by

$$\tau^2 = \frac{1}{\delta} \{ (\delta+1) - \sqrt{4\delta+\epsilon} \}$$

so that  $\tau$  becomes complex when

$$(\delta+1) < \sqrt{4\delta+\epsilon}$$

The transition from a stable to unstable regime for the internal gravitational modes is then given by the condition

$$1 - \sqrt{\epsilon} < \delta < 1 + \sqrt{\epsilon} \quad (3.5)$$

When  $\delta$  is in the range given by (3.5), we obtain instability and outside this range we have stability. This is a rather interesting result because it shows that after obtaining instability at a certain critical value of the shear represented by the lower limit  $1-\sqrt{\epsilon}$ , we once again go back to a stable regime after the shear reaches another critical value

represented by the upper limit. The result is in contrast to what one obtains in the case of a two-fluid system with a rigid top (or the filtered system with free surface). The primary difference between the model with a rigid top and one with a free surface is the absence of the external or free surface-gravitational modes in the case of the former model. Consequently the difference between the stability character of the two models may be ascribed to the presence of the external modes with consequent stabilizing effect of the divergence associated with a free surface. The stability diagram corresponding to the criteria (3.3) to (3.5) is shown in Fig. 1.

Case (b): With rotation

Let us now turn our attention to cases with rotation and introduce the following approximation.

$$\gamma_1 = \gamma_2 = \frac{2}{1-\epsilon} \quad (3.6)$$

which implies that  $\epsilon \bar{U}_2 - \bar{U}_1 \approx \bar{U}_2 - \bar{U}_1$ , which is a reasonable approximation since  $\epsilon \approx 1$  for most practical purposes. The characteristic equation (2.3) then reduces to

$$\begin{aligned} & [\delta(1+\tau)^2 - (1+\lambda)] [\delta(1-\tau)^2 - (1+\lambda)] (1-\tau^2) \\ & + \gamma\lambda \{ [\delta(1+\tau)^2 - (1+\lambda)] (1+\tau) + [\delta(1-\tau)^2 - (1+\lambda)] (1-\tau) \} \\ & + \gamma^2 \lambda^2 (1-\epsilon) - \epsilon (1-\tau^2) + 2\epsilon\gamma\lambda = 0. \end{aligned} \quad (3.7)$$

Case (b1): Rotational mode (quasi-geostrophic) instability

In the normal case of a physical system containing rotational and gravitational modes, the quasi-geostrophic approximation which is used to filter out the gravitational modes is

$$\delta(1+\tau)^2 \ll (1+\lambda). \quad (3.8)$$

On using this approximation along with the definition of  $\gamma$  given in

(3.6) equation (3.7) reduces to

$$[(1+\lambda)^2 - \epsilon] \tau^2 = [(1-\lambda)^2 - \epsilon]. \quad (3.9)$$

Equation (3.9) then shows that instability is realised for all wave lengths.

$$1 - \sqrt{\epsilon} < \lambda < 1 + \sqrt{\epsilon} \quad (3.10)$$

From the definition of  $\lambda$ , we see that  $\lambda$  is proportional to wave length of the perturbations. Hence the lower limit of (3.10),  $\lambda = 1 - \sqrt{\epsilon}$  represents the short wave cut-off for instability corresponding to Eady's (1949) cut off. For reasonable values of  $\epsilon$  and depth  $D$ , like

$$\epsilon = 0.98, \quad D = 5 \text{ km}, \quad f = 10^{-4} \text{ sec}^{-1}$$

we see that the cut off on the short wave length side corresponds (with the perturbation wave-number of the y-direction equal to zero) to a wavelength  $L (= 2\pi/k)$  of

$$L \approx 1400 \text{ km.}$$

Equation (3.10) also shows that there is cut-off to instability on the long wave side. This result is analogous to the result obtained by Phillips (1951) with a two-layer rigid top model. As Phillips pointed out in his paper the reason Eady does not obtain a cut off on the long wave length side is due to a certain approximation introduced by Eady.

Case (b2): Rotational-gravitational mode instability

We have so far considered the effect of the traditional quasi-geostrophic approximation (3.8). This approximation removes both the external and internal gravitational modes from the characteristic equation (3.7). Since the phase speeds of the internal gravitational modes are dependent on modified gravity  $g(1-\epsilon)$  rather than  $g$  itself, these modes usually propagate with a speed much smaller than the

external modes. As a matter of fact, the values of  $c$  for some of the internal gravitational modes are of the same order of magnitude as those for rotational modes. Consequently, the quasi-geostrophic approximation as stated in (3.8) is too stringent. For this reason, we consider now the next order of approximation.

$$\delta^2(1-\tau^2)^2 \ll (1+\lambda)^2 \quad (3.11)$$

This approximation may be shown to be equivalent to suppressing only the solutions corresponding to the external gravitational modes, (see also case a1) leaving the internal gravitational modes and the rotational modes in the system. Introduction of approximation (3.11) into equation (3.7) results in the bi-quadratic equation:

$$2\delta(1+\lambda)\tau^4 - [(1+\lambda)^2 - \epsilon - 6\delta\lambda\gamma]\tau^2 + [(1-\lambda)^2 - \epsilon - 2\delta(1+\lambda-\lambda\gamma)] = 0$$

The solution to the above equation may be written as:

$$\tau^2 = \frac{2}{a} [b \pm \sqrt{b^2 - ad}] \quad (3.12)$$

where

$$a \equiv 8\delta(1+\lambda)$$

$$b \equiv (1+\lambda)^2 - \epsilon - 6\delta\lambda\gamma$$

$$d \equiv (1-\lambda)^2 - \epsilon - 2\delta(1+\lambda - \lambda\gamma)$$

A numerical analysis of equation (3.12) is carried out for the following values of basic state quantities:

$$\epsilon = 0.98, D_1 = D_2 = 5 \text{ km}, f = 10^{-4} \text{ sec}^{-1}, g = 9.8 \text{ msec}^{-2}.$$

An examination of the equation (3.12) immediately reveals the following possibilities:

Table 1. Classification of stable and unstable regimes

Case	d	b	$b^2 - ad$	No. of unstable modes
(i)	<0	>0	>0	2
(ii)	>0	<0	>0	4
(iii)	>0	>0	>0	0
(iv)	>0	<0	<0	4

In the preceding classification, there is an important difference between the unstable modes obtained in cases (i), (ii), on one hand and case (iv) on the other hand. The unstable modes belonging to cases (i) and (ii) are characterised by having a zero real part for  $\tau$  - that is,  $\tau_r = 0$  for the two (or four) unstable roots of  $\tau$ . This then means that the perturbations belonging to this class are propagated with a mean speed  $c_r = \bar{U} \equiv \frac{1}{2}(\bar{U}_1 + \bar{U}_2)$  in dimensional form. The unstable modes belonging to case (iv) however, are characterised by  $\tau_r \neq 0$  for all four unstable modes. It will be shown shortly that these unstable modes of case (iv) result from an interaction between the gravitational and rotational modes and consequently this instability may be termed the "mixed mode instability" (see Rao and Simons 1969).

The regions of stability and instability obtained from equation (3.12) are shown in Figure 2 on a  $\delta - \lambda$  plane. The  $\lambda = 0$  axis corresponding to the no rotation case and the instabilities obtained along this axis, consequently, must be gravitational instabilities. One can see from equation (3.3) that this instability is obtained for values of  $\delta > 0.01$ . The value  $\delta = 0.01$  corresponds to a transition from case (iii) to case (i) associated with equation (3.12). In the region  $\delta > 0.01$  and  $\lambda < 0.01$ ,

the instabilities are those of the gravitational modes. The quasi-geostrophic instabilities are those along the  $\delta = 0$  axis. Since  $\delta$  exactly equal to zero implies a zero shear which is then a case of no instability, one should view  $\delta = 0$  as a limiting case for pure geostrophic instabilities. Then we have instabilities of the rotational modes between the values of  $\lambda$  as given by equation (3.10). These instabilities again represent a transition from case (iii) to case (i). The instabilities obtained in the range  $\delta < 0.01$  and  $\lambda > 0.01$  primarily represent the instabilities of the rotational modes. The transition from the region of gravitational instabilities ( $\delta > 0.01$ ,  $\lambda < 0.01$ ) to rotational instabilities ( $\delta < 0.01$ ,  $\lambda > 0.01$ ) seems to be gradual, and in the vicinity of  $\delta = 0.01$  and  $\lambda = 0.01$ , it is not possible to state positively whether the instability is due to rotational or gravitational modes. In the region  $\delta > 0.01$  and  $\lambda > 0.01$  we obtain a region where the rotational modes and the gravitational modes are independently unstable. This unstable region corresponds to case (ii) and represents modes with  $\tau_r = 0$ . As  $\lambda$  increases, this region extends towards lower values of  $\delta$  as shown on the right side of Figure 2.

The area denoted by vertical hatching in Figure 2 represents what are called the mixed mode instabilities belonging to class (iv). These mixed mode instabilities may be viewed as a primary consequence of relaxing the rather rigid quasi-geostrophic approximation. The modification of the growth rates of the rotational modes as well as the presence of pure gravitational instabilities are also consequences of the non-geostrophic nature of the problem.

The mixed mode instabilities occur in an enclosed region in the area  $\delta, \lambda < 0.01$  and also in a rather small area for  $\lambda > 1$ . The region of mixed mode instability is enclosed by the curve  $b^2 - ad = 0$  in the  $\delta, \lambda$  - plane.

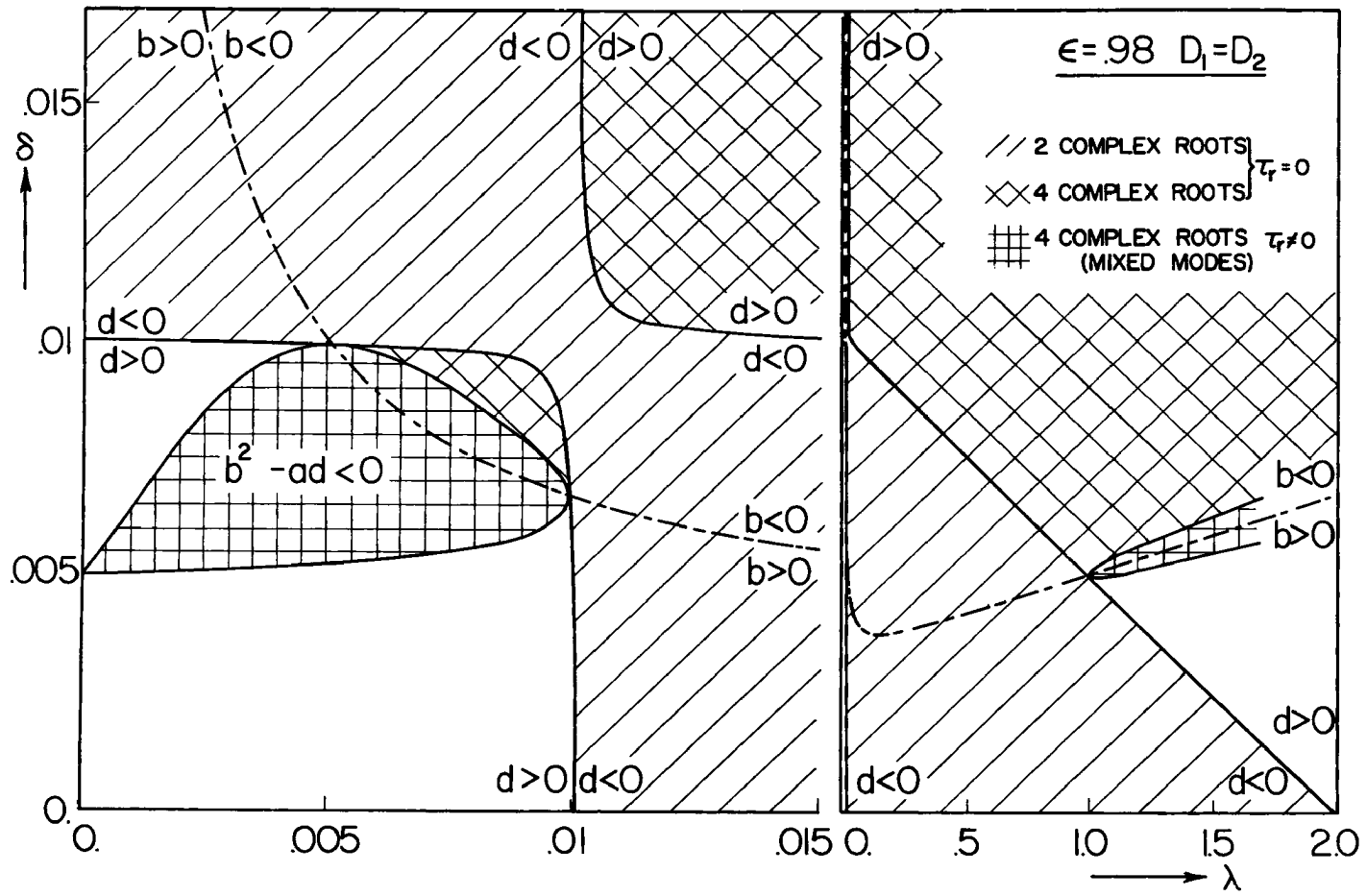


Figure 2. Stability diagram for the rotating case.  $\lambda$  is proportional to wave length square and  $\delta$  to the square of shear.

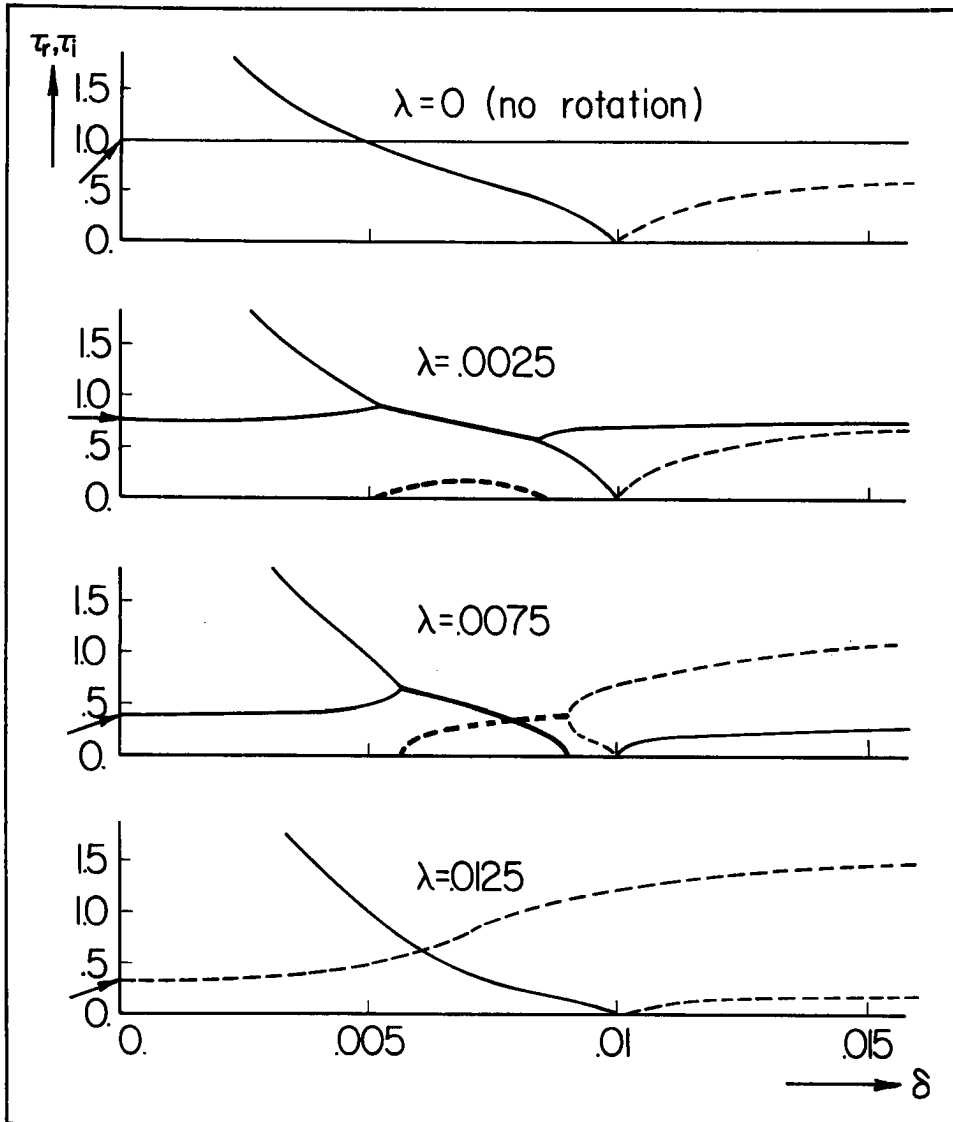


Figure 3. Schematic representation of the changes of  $\tau_r$  (solid lines),  $\tau_i$  (dashed lines) as a function  $\delta$  for various wave lengths. Arrow indicates quasi-geostrophic solution ( $\delta \ll 1$ ).

The unstable modes in this case are characterised by having  $\tau_r \neq 0$  and as will be shown below, they result from a coalescence of gravitational and rotational modes.

The nature of the instabilities presented in Figure 2 may be elucidated by a careful tracking of the unstable modes as the shear (or  $\delta$ ) or the wavelength (or  $\lambda$ ) is increased. For this purpose we consider the behaviour of various modes taken along a line of constant  $\lambda$  as a function of  $\delta$ . This process is illustrated in Figure 3. The top diagram in Figure 3 is taken along the line  $\lambda = 0$ . This then corresponds to the case of no rotation with only the gravitational modes being unstable. The rotational modes in this case are stable and are simply given by  $\tau = \pm 1$  for all  $\delta$ . We see that as  $\delta$  is increased, the  $\tau_r$  of the gravitational mode decreases until it becomes zero at  $\delta = 0.01$ . During this time, the other member of the gravitational mode pair which is in the negative half of the  $\tau$ -axis (not shown in this diagram) also will have its  $\tau_r \rightarrow 0$  as  $\delta \rightarrow 0.01$ . Then at  $\delta = 0.01$ , both the gravitational modes meet at  $\tau_r = 0$  and initiate instability, the intensity of which is then measured by  $\tau_i$  given by the dotted line. It should be noted that corresponding to the positive  $\tau_i$  shown here, there is a negative  $\tau_i$  of the same magnitude which again is not shown here. In any case, we see that for  $\lambda = 0$ , the gravitational modes meet each other and become unstable, while the rotational modes remain unchanged as  $\delta$  changes.

The second picture from top in Figure 3 represents the conditions along the line  $\lambda = 0.0025$ . Here we can recognise the gravitational and rotational modes for small values of  $\delta$  by a comparison with the picture above. As  $\delta$  is increasing, the gravitational and rotational modes come together at a value of  $\delta$  slightly greater than 0.005 to produce

instability. By comparison with Figure 2 we see that this instability is in the region of mixed mode instability. The imaginary component  $\tau_i$  which is developed when the gravitational and rotational modes came together is again indicated by the dotted line. Note that the same process has occurred in the meantime in the half plane for negative  $\tau$  which is not shown here. Thus at this time there are four complex  $\tau$ 's, all of which have non-zero real parts  $\tau_r$ , i.e. case (iv) of Table 1. As  $\delta$  is increases, the  $\tau_r$  of the mixed gravity-rotational mode changes until another value of  $\delta$  is reached where we pass into a stable region. At this point  $\tau_i$ , of course, goes to zero and the gravitational and rotational modes separate again. Again by comparison with the picture corresponding to  $\lambda = 0$ , we see that the gravitational mode is approaching  $\tau_r = 0$  as  $\delta$  increases and the rotational mode is tending towards its asymptotic value. At  $\delta = 0.01$ , the gravitational mode meets its counterpart coming from below the axis at  $\tau_r = 0$  and we now obtain pure gravitational instability with  $\tau_r = 0$  and  $\tau_i$  given by the dashed line.

The third picture from the top in Figure 3 is taken along  $\lambda = 0.0075$ . Once again by comparison with preceding curves, we see that mixed mode instability is obtained at a value of  $\delta = 0.0056$ . As  $\delta$  increases, the  $\tau_r$  of the mixed mode approaches zero and at  $\delta = 0.009$  the mixed mode coming from above meets the mixed mode coming from below at  $\tau_r = 0$ . From  $\delta = 0.009$  to  $\delta = 0.01$  we have four unstable modes with  $\tau_r = 0$ , which would then correspond to case (ii) of Table 1. For  $\delta > 0.01$ , the rotational modes become stable and as  $\delta$  increases, their  $\tau_r$ 's approach their asymptotic value while the gravitational pair remains unstable with  $\tau_r = 0$  and  $\tau_i \neq 0$ .

Finally when  $\lambda = 0.0125$  and for small  $\delta$  we have rotational mode

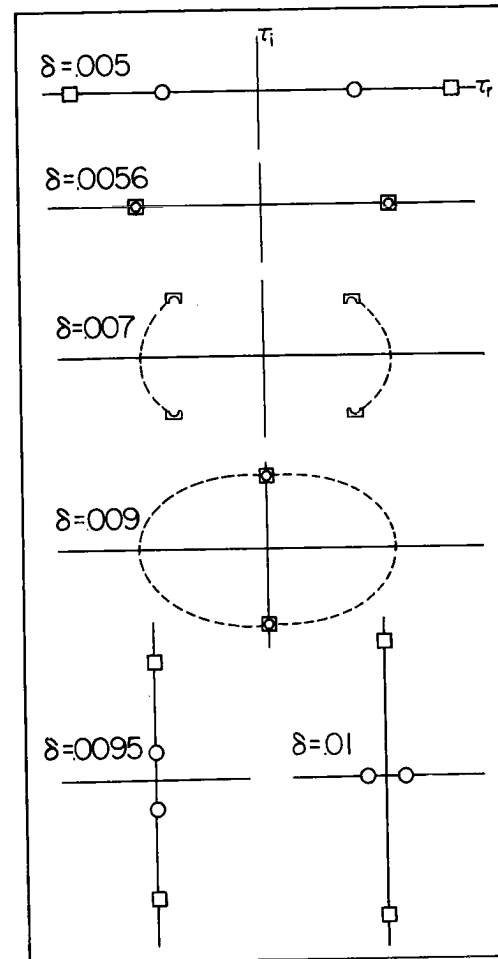
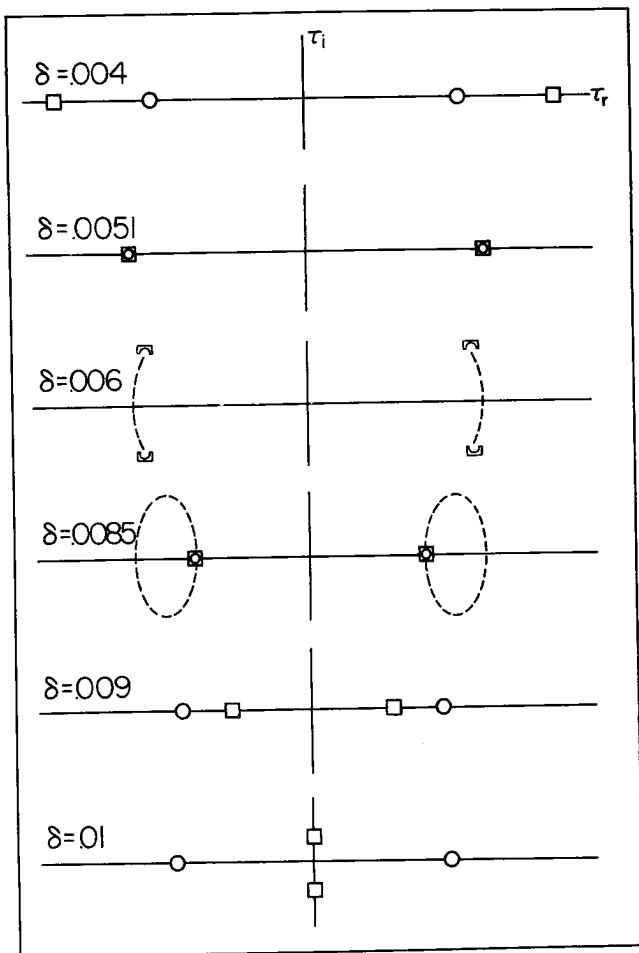


Figure 4. Schematic representation of the changes of characteristic value  $\tau$  on a complex  $\tau$ -plane for  $\lambda = 0.0025$  (left) and for  $\lambda = 0.0075$  (right) at various values of  $\delta$ .

instability with  $\tau_r = 0$ . The gravitational modes in this case are stable until  $\delta = 0.01$  is reached. At that value, the gravitational modes become unstable by themselves with  $\tau_r = 0$  and  $\tau_i \neq 0$ . This is case (ii) of Table 1.

Figure 4 illustrates the instability mechanism on a complex  $\tau$  - plane at various values of  $\delta$ . In Figure 4, the left panel is for  $\lambda = 0.0025$  and the right panel is for  $\lambda = 0.0075$ . In these figures the squares represent the gravitational modes and the circles represent the rotational modes. The half-circles-plus-squares represent the mixed modes. In each figure the mixed mode instability (case iv of Table 1) is represented by the third diagram, and the pure gravitational mode instability (case i of Table 1) by the last diagram. The one before the last diagram of the right panel of Figure 4 is an example of case (ii) of Table 1, i.e., rotational modes independent of one another.

#### 4. Summary and Conclusions

The problem of dynamic stability of a two-fluid system with a free surface has been examined. When there is no rotation, one obtains the Kelvin-Helmholtz type instability of the gravitational modes. The analysis shows that in the case of a free surface model with external gravitational modes present, the fluid configuration becomes unstable when a critical value of shear is reached and becomes stable again at higher values of shear. This result is in contrast to that obtained in the case of a rigid top model or the case where the external modes are filtered out in the free surface model. In both these cases, once instability is initiated by the shear reaching a critical value, the instability persists for all higher shears.

Next the case of constant rotation is considered. In this case,

the depth of each fluid layer is treated as a constant except when differentiated. An additional approximation is introduced in the equation for the slope of the interface in which the term  $(\epsilon \bar{U}_2 - \bar{U}_1)$  is replaced by  $(\bar{U}_2 - \bar{U}_1)$  where  $\epsilon$  is the density ratio of the two fluids and  $\bar{U}_2, \bar{U}_1$  are the speeds of the fluid layers in the basic state. If the uniform depths of the layers are assumed to be equal and the external gravity modes are filtered out then the characteristic equation reduces to a bi-quadratic. From an analysis of this bi-quadratic equation, a stability diagram is constructed on a wave length - shear plane. It shows that the stability diagram consists of regions where only the gravitational modes are unstable (large shears, small wavelengths), only the rotational modes are unstable (small shears, large wavelength), both the rotational and gravitational modes are independently unstable (large shears, large wavelengths) in addition to regions where the instability is generated by an interaction between the rotational and gravitational modes (primarily in the range of moderate shears and wavelengths). The latter type of instability is called the "mixed mode" instability and represents a unique feature of the non-geostrophic nature of the stability problem.

An analysis has also been made using the complete characteristic equation derived in section 2. The results show no significant difference in the stability character as deduced from the bi-quadratic equation. Similar results are also obtained from an analysis of the rigid top model, which gives a quartic equation under the same approximations as stated above, instead of a bi-quadratic equation. The mixed mode instabilities are also realised in a numerical treatment of the problem in a channel, where the depth variations are taken into account and all modes of

oscillation are retained in the problem (Rao and Simons 1969). From these considerations it appears very plausible that mixed mode instabilities are obtained in regions where neither the pure Kelvin-Helmholtz instabilities nor the pure geostrophic instabilities are dominant.

REFERENCES

- Chandrasekhar, S. 1961: Hydrodynamic and Hydromagnetic Stability.  
Oxford-Clarendon Press.
- Eady E. 1949: Long Waves and Cyclone Waves. Tellus 1, 33-52.
- Godske, C. L., T. Bergeron, J. Bjerknes, R. C. Bundgaard 1957: Dynamic  
Meteorology and Weather Forecasting. American Meteorological Society,  
Boston, Mass., 800 pp.
- Phillips, N. A. 1951: A Simple three-dimensional model for the study  
of large-scale extratropical flow patterns. Journal of Meteorology,  
8, 381-394.
- Rao, Desiraju B. and T. J. Simons 1969: Stability of a sloping interface  
in a rotating two-fluid system. Atmospheric Science Paper No. 151,  
Colorado State University, 37 pp.